Role of the β4Thr−β73Asp Hydrogen Bond in HbS Polymer and Domain Formation from Multinucleate-Containing Clusters†

Kazuhiko Adachi,*,‡ Min Ding,‡ and Saul Surrey§

The Children's Hospital of Philadelphia Division of Hematology, University of Pennsylvania School of Medicine, Philadelphia, Pennsylvania 19104, and Cardeza Foundation for Hematologic Research, Department of Medicine, Jefferson Medical College, Philadelphia, Pennsylvania 19107

Received January 25, 2008; Revised Manuscript Received March 19, 2008

ABSTRACT: Fiber formation and domain formation from deoxy-HbS as well as from β4 and β73 HbS variants were investigated after temperature jump using DIC microscopy to gain a basic understanding of the determinants involved. Oversaturated deoxy-HbS generated numerous 14-stranded fibers and formed ovoid-shaped, multispherulitic domains. Domain number increased linearly as a function of time. Oversaturated deoxy-$\alpha_2\beta_2^{E6V,T4S}$ also generated time-dependent, ovoid-shaped spherulitic domains like HbS and $\alpha_2\beta_2^{E6V,D73H}$ in the deoxy form. In contrast, $\alpha_2\beta_2^{E6V,T4Y}$ and HbC-Harlem ($\alpha_2\beta_2^{E6V,D73N}$) in the deoxy form generated time-dependent, ball-shaped domains containing many straight, crystalline-like fibers without evidence of branching. Some of these domains formed large needlelike crystals after overnight incubation. The inhibitory effect on polymer formation by β4Tyr in HbS was stronger than that by β4Ser but weaker than that by β73Asn or β73Leu. In contrast, both deoxy- and oxy-$\alpha_2\beta_2^{E6V,T4V}$ promoted formation of tiny, disordered amorphous aggregates without a delay time like oxy-HbS, which is in contrast to formation after a delay time of needlelike fibers for $\alpha_2\beta_2^{E6V,D73L}$. Solubilities for both deoxy- and oxy-$\alpha_2\beta_2^{E6V,T4V}$ were similar to that of deoxy-$\alpha_2\beta_2^{E6V,D73H}$ but ∼10-fold lower than that of deoxy-HbS. These results suggest that the strength of the hydrogen bond between β4Thr and β73Asp and the balance between the hydrogen bond and β6Val hydrophobic interactions in deoxy-HbS polymers control formation of different types of fibers in a single domain or lead to formation of disordered, non-nucleated amorphous aggregates. These results also lead to a model in which multinucleation rather than a single-nucleation event occurs in a single cluster to generate numerous fibers growing from a single domain.

Replacement of β6Glu with a hydrophobic Val in the β chain of hemoglobin (HbS)[1] leads to the formation of long, multistranded polymers when HbS is deoxygenated (*1, 2*). Intracellular polymers or fibers cause a significant reduction in RBC deformability (sickling), obstructing flow in the microcirculation in patients with sickle cell disease (SCD) (*1, 2*). Oversaturated deoxy-HbS aggregates after nucleation and forms long, multistranded polymers, which are comprised of 14-stranded fibers rather than stable double-stranded crystals. The fibers are 21 nm in diameter and are rodlike, twisted strands of HbS molecules stabilized by well-defined intra-double-strand interactions (*2*). Each is composed of seven half-staggered double strands (*3*), and this double-stranded structure of deoxy-HbS fibers within red blood cells of patients with SCD may be similar to that of deoxy-HbS crystals in vitro. Details of the deoxy-HbS crystal structure are known, permitting a structural comparison with crystals of deoxy-HbA (*4, 5*). However, even though polymer assembly of oversaturated deoxy-HbS is thermodynamically similar to crystallization (*2*), the reason why HbS quickly forms 14-stranded fibers rather than the more stable double-stranded crystals is not clear. We previously reported that both HbC-Harlem, a naturally occurring HbS variant with two amino acid changes (β73Asp to Asn and β6Glu to Val), and recombinant $\alpha_2\beta_2^{E6V,D73L}$ inhibited polymerization and formed straight, crystalline-like fibers instead of the twisted 14-stranded fibers present in deoxy-HbS (*6, 7*). The much longer delay time prior to polymerization and the formation of double-stranded fibers for HbC-Harlem and likely for $\alpha_2\beta_2^{E6V,D73L}$ were suggested to be caused by weakening of the hydrogen bond interaction between the β4 and β73 amino acids in HbS polymers (*7*). In contrast, a change to β73His in HbS promoted polymerization of fibers and domain formation characterized by fiber morphology similar to that of 14-stranded fibers of deoxy-HbS, possibly caused by facilitation of the hydrogen bond interaction between β73His and β4Thr (*7*). These polymerization properties of HbS indicate that the β4Thr−β73Asp hydrogen bond in addition to β6Val hydrophobicity plays a significant role in double- versus 14-stranded fiber growth following domain formation of HbS polymers.

† This research was supported in part by grants from the National Institutes of Health (HL70596, HL69256, and DK61692) and the Cardeza Foundation for Hematologic Research.

* To whom correspondence should be addressed: Division of Hematology, The Children's Hospital of Philadelphia, 34th St. and Civic Center Blvd., Philadelphia, PA 19104. Telephone: (215) 590-3576. Fax: (215) 590-4834. E-mail: adachi@email.chop.edu.

‡ University of Pennsylvania School of Medicine.

§ Jefferson Medical College.

[1] Abbreviations: HbS, sickle hemoglobin ($\alpha_2\beta_2^{E6V}$); HbC-Harlem, hemoglobin C-Harlem ($\alpha_2\beta_2^{E6V,D73N}$); SCD, sickle cell disease; RBC, red blood cell; DIC, differential interference contrast; CCD, charge-coupled device.

10.1021/bi800149u CCC: $40.75
Published on Web 04/18/2008

The vaso-occlusive manifestations of SCD are related to the kinetics of deoxy-HbS polymer formation (*2*). The kinetics of polymerization of oversaturated deoxy-HbS is characterized by a marked delay period prior to polymerization followed by a dramatic and autocatalytic increase in the level of polymer formation (*2*). This process has been explained by a mechanism whereby polymers first form single homogeneous nuclei followed by fiber formation after which heterogeneous nuclei attach to these formed fibers (*2, 8, 9*). After nucleation, monomers of deoxy-HbS bind to nuclei to form polymers, and each polymer assembles into 14-stranded fibers, which then form a viscous gel (*3, 10*). Fibers are typically found in regions called domains during their elongation, and heterogeneous nuclei attach to the polymer resulting in branched growth of fibers (*11*). Earlier electron microscopy studies showed radially oriented fibers of deoxy-HbS (*12*). Linear dichroism and birefringence measurements of a large domain showed a rather uniform density, with polymers oriented along the radius of each domain (*13*). A relationship between rates of domain formation and the kinetics of polymerization or gelation of deoxy-HbS also was experimentally and theoretically established (*2, 9*).

In addition, growth of domains, development of HbS polymers, and details of their structure have been studied by differential interference contrast (DIC) microscopy (*14, 15*). After nucleation, domains show extensive growth followed by heterogeneous nucleation which becomes visible as branching (*15*). Deoxy-HbS polymerization kinetics observed by DIC microscopy also indicates that domain structure depends on the kinetics of formation of nuclei (*15*). More recently, DIC microscopy of deoxy-HbS fibers after laser photolysis showed a number of domains, each including many fibers (*16*), and that these time-dependent, spherulitic domains were made from homogeneous nuclei during phase transition (*16, 17*). These studies suggested that homogeneous nucleation prior to HbS polymer formation occurs in a single liquid cluster, which represents a precursor phase during liquid to solid phase transition of oversaturated deoxy-HbS. These theoretical analyses of nuclei and domain formation are based on the assumption that each domain is generated by a single primary nucleation event as in the process of crystal formation by nuclei (*18*). However, domain formation of HbC-Harlem and $\alpha_2\beta_2^{E6V,D73L}$ is time-dependent as with HbS and characterized by ball-shaped domains each containing numerous needlelike crystalline fibers with no apparent branching (*7, 19*).

An understanding of the initiation of polymerization, including the process of multifiber formation in a single domain containing double- or 14-stranded fibers of HbS or its variants, based on protein−protein interactions of HbS polymers is critical to gaining a full understanding of polymer formation in SCD and in designing structure-based anti-HbS polymerization hemoglobins and peptides (*20, 21*). This knowledge also may improve our understanding of diseases in which protein fibers are formed (e.g., cataracts, Alzheimer's, Huntington's, and prion diseases) (*17, 22*−*24*). This report evaluates the effects of site-directed mutations at the β4 and/or β73 site in deoxy-HbS polymers on formation of domains associated with fiber formation. The temperature-jump method was used to initiate polymerization in vitro, and DIC microscopy was employed to define polymer formation. Finally, the dependency of β6Val hydrophobic and β4Thr hydrogen bond interactions in oversaturated deoxy-HbS and deoxy-HbC-Harlem monomers on formation of different types of clusters, each containing numerous nuclei leading to formation of double- or 14-stranded fibers growing from a single domain, is addressed.

EXPERIMENTAL PROCEDURES

HbS and HbC-Harlem were purified from blood donors with AS and HbAC-Harlem, respectively, as previously described by standard chromatography on a Source 15S FPLC column (Pharmacia Biotech, Inc., Piscataway, NJ) equilibrated with 40 mM Bis-Tris buffer (pH 5.8) and eluted using a linear gradient from 0 to 0.2 M NaCl in the same buffer (*19*). Recombinant $\alpha_2\beta_2^{E6V,T4S}$, $\alpha_2\beta_2^{E6V,T4Y}$, and $\alpha_2\beta_2^{E6V,T4V}$ were expressed in bacteria after the corresponding cDNAs were subcloned into pHE2, which coexpresses α- and β-globin chains as well as methionine aminopeptidase under transcriptional control of a ptac promoter (*25*). β-Globin chain variants were constructed by site-specific mutagenesis of normal β chain using recombination/polymerase chain reaction (PCR), as described previously (*7, 26*), and were coexpressed with α chains to form tetrameric HbS variants (*7*). Purification of hemoglobin was as described previously (*7*), and sample purity was assessed by cellulose acetate electrophoresis on Titan III membranes at pH 8.6 with Super-Heme buffer, using HPLC and SDS−PAGE. Electrospray ionization mass spectrometry was performed on the purified recombinant HbS variants using a VG BioQ triple-quadrapole mass spectrometer (Micromass, Altrincham, Cheshire, U.K.) to confirm expected molecular masses. Data analysis employed MassLynx (Micromass, Altrincham) (*7*). Hemoglobin concentrations were determined spectrophotometrically using a millimolar extinction coefficient mE_{555} of 50 for deoxyhemoglobin and mE_{579} of 53.6 for carbonmonoxyhemoglobin (on a tetramer basis). Purified hemoglobins were stored in the CO-liganded form at −80 °C until they were used. Hemoglobin solutions were concentrated using a centricon centrifugal concentrator with a membrane cutoff of 30000 Da (Centriprep, Milipore Co., Bedford, MA). Oxyhemoglobin was prepared by first blowing oxygen across the surface of a CO-HbS solution in a rotary evaporator under a 150 W flood-light bulb in an ice bath for ~1 h.

Fiber formation by deoxy and oxy forms of HbS and HbS variants was evaluated by DIC microscopy and was initiated on glass slides by addition of phosphate buffer (pH 7.4) containing sodium dithionite to oxy-HbS solutions in 0.1 M phosphate buffer (pH 7.4) at 4 °C. The final phosphate concentration was 0.1 or 1.0 M (pH 7.4), with 100 mM sodium dithionite (*7*). One or two microliters of solution was pipetted onto a glass slide which then was sealed with an 18 mm square coverslip using Mount-Quick solution (Daido Sangyo Co., Ltd., Tokyo, Japan) (*7*), or the solution was inserted into a glass capillary tube (30 μm path length × 0.3 mm width with a length of 50 mm) (Dynamics, Inc., Rockaway, NJ) by capillary action. Both ends of the tube were sealed by Mount-Quick solution, and the tube was mounted on the glass slide after a 1 h incubation on ice. Polymer or fiber formation of deoxygenated hemoglobin using coverslips sealed on a glass slide or sealed capillary tubes was induced by a temperature jump from 0 °C on ice

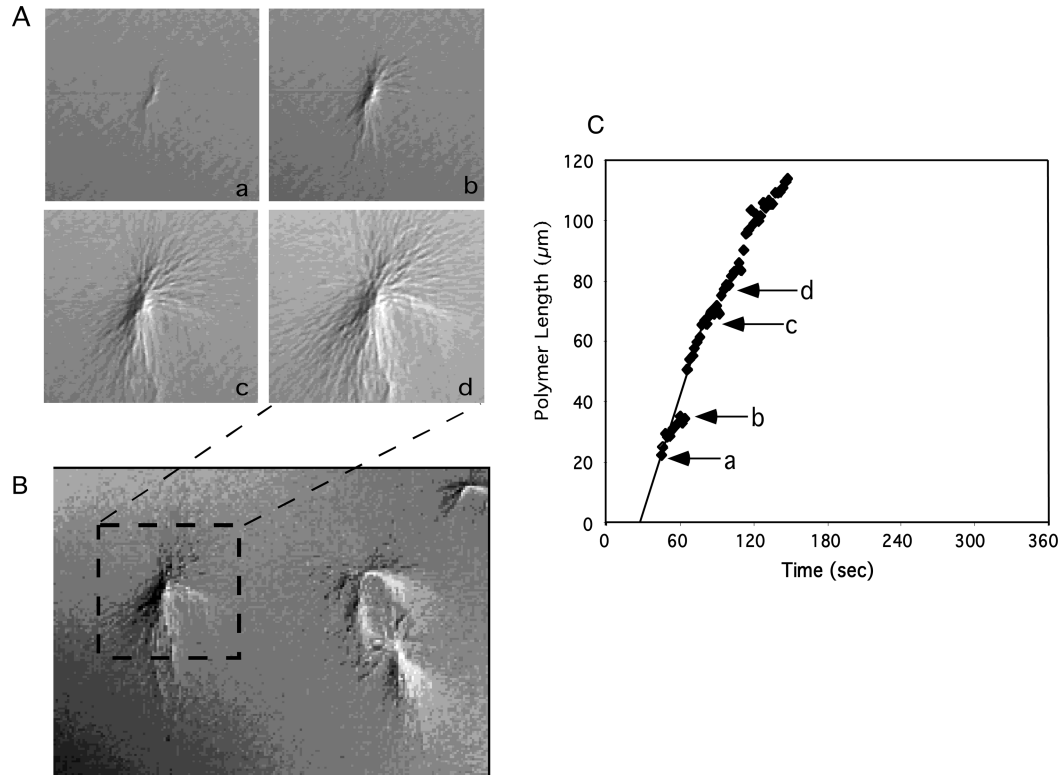

FIGURE 1: Time course and growth of deoxy-HbS fibers in 0.1 M phosphate buffer using DIC microscopy. (A) DIC images of growth of deoxy-HbS fibers at 21.9 g/dL as a function of time in 0.1 M phosphate buffer after a temperature jump from 0 °C to room temperature (22 °C) were recorded on an image grabber board of a computer. Panels a−d represent images taken at 45, 64, 82, and 110 s, respectively. (B) DIC images of elongated fibers in multidomains in an area of 116 μm × 153 μm after 110 s. (C) Growth of fibers in a single domain calculated from DIC images by counting pixel number (fiber length) as a function of time.

to room temperature (~22 °C). The total mass of polymer in a domain was analyzed by DIC microscopy by measuring the pixel area of a single domain using an Olympus microscope equipped with DIC optics and a 40× (1.00 NA) immersion lens. The microscopic images obtained were transferred to a personal computer via an image grabber board (Universal Image Corp., Downingtown, PA) and a CCD (charge-coupled device) camera (Cohu Camera, Cohu, Inc., San Diego, CA) (*6, 7*). To measure the area and length of polymer fibers, images were taken of a hemocytometer with 50 μm divisions (American Optical Corp., Buffalo, NY) at a magnification of 400×. Using the line measurement tool in the Molecular Device Image Analysis System (Universal Image Corp.), we determined the length or area of the polymer domain containing fibers by counting pixel number. Kinetics of polymerization and solubility of HbS and HbS variants were evaluated in 1.0 M phosphate buffers (pH 7.4) at 22 °C (*7*), and solubility was determined by centrifugation after completion of polymerization as measured by turbidity.

RESULTS

Using DIC microscopy, we observed polymerization and domain formation of oversaturated deoxy-HbS after a delay time in 0.1 M phosphate buffer at 22 °C following a temperature jump after preincubation for 1 h on ice. When concentrations of deoxy-HbS greater than its solubility (~17 g/dL) are used, many HbS fibers and/or bundles form that include both straight and bent fibers. When concentrations of deoxy-HbS of >25 g/dL are used, deoxy-HbS rapidly polymerizes without a measurable delay time prior to formation of spherulitic domains that can be monitored by DIC microscopy. In contrast, after the temperature jump, deoxy-HbS at 17−22 g/dL forms fibers in spherulitic domains after a delay time. Thus, we observed deoxy-HbS fiber formation at 21.9 g/dL, as shown in Figure 1. Formation and growth of fibers in spherulitic domains occurred after a delay time of 1 min. The delay time prior to polymerization and domain formation depends on temperature in addition to deoxy-HbS concentration. Furthermore, the length of the delay time and rates of domain formation depend on amounts of solution per unit space under a coverslip sealed to a glass slide; the higher the volume of solution, the faster domain formation and the greater the number of domains. Many fibers continue to grow from a central region to form a single domain. Almost all polymers contain tightly packed fibers with the highest polymer density at the center from which fibers grow outward. Using the temperature-jump method, we found that fibers grew at a rate of 1.21 ± 0.25 μm/s (Figure 1), and the total length of polymers generated in 0.1 M phosphate was >60 μm, with some reaching 120 μm within 5 min.

Our previous study showed that amounts of HbS and HbS variants in the deoxy form required for polymerization and domain formation in 1.0 M phosphate buffer were reduced compared to those required in 0.1 M phosphate buffer (e.g., ~3, 9, and 16 g/dL in 1.0 M phosphate buffer instead of 20, 42, and 50 g/dL for HbS, HbC-Harlem, and $\alpha_2\beta_2^{E6V,D73L}$ in 0.1 M phosphate buffer, respectively) when using hemoglobin solutions under a sealed coverslip mounted to a glass slide (*7*). To compare results of polymerization of HbS β4 variants with those of HbS β73 variants, we studied polymerization and domain formation of oversaturated

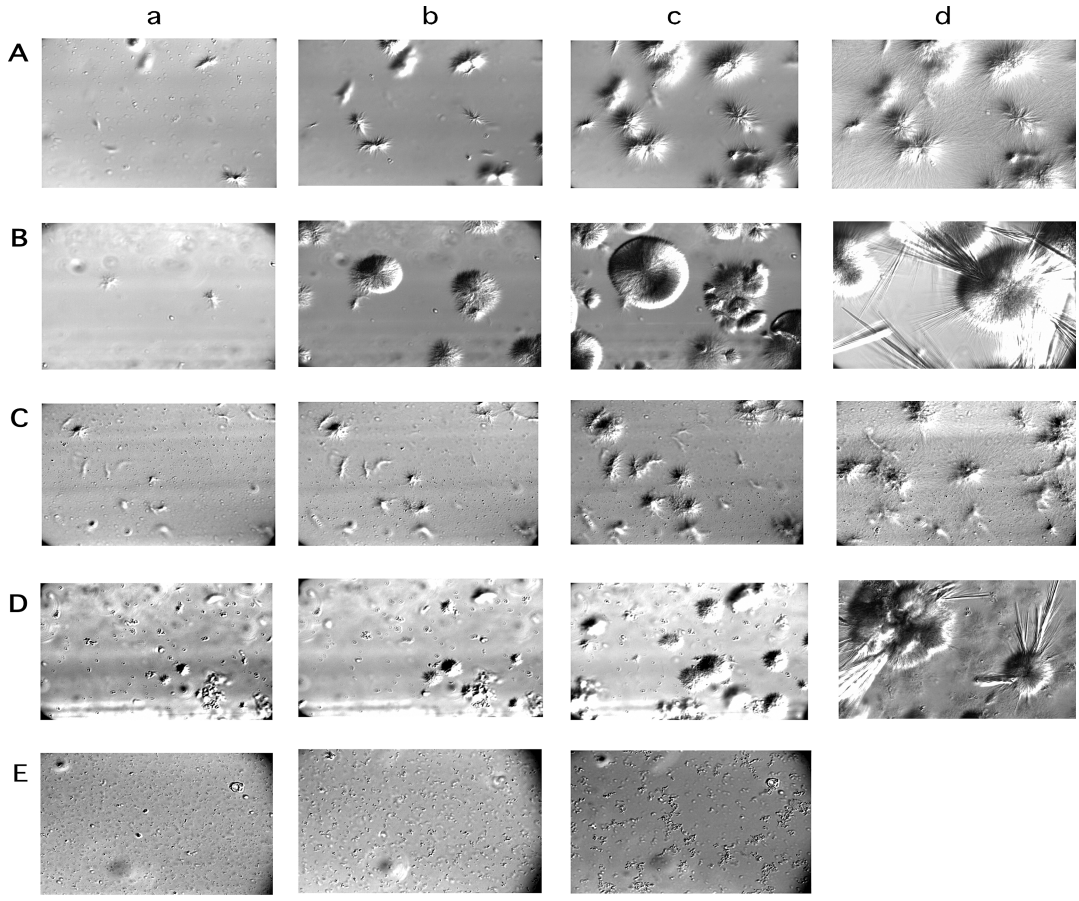

FIGURE 2: DIC images of fiber and domain size for deoxy-HbS as well as for HbS β73 and β4 variants in the deoxy form as a function of time. Rows A−E represent DIC images as a function of time of polymerized fibers and domains of HbS (3.0 g/dL), HbC-Harlem (6.1 g/dL), $\alpha_2\beta_2^{E6V,T4S}$ (3.0 g/dL), $\alpha_2\beta_2^{E6V,T4Y}$ (4.0 g/dL), and $\alpha_2\beta_2^{E6V,T4V}$ (0.5 g/dL) in the deoxy form in 1.0 M phosphate buffer at pH 7.4 after a temperature jump to 22 °C. Images of each frame represent an area of 190 μm × 125 μm. Row A (HbS) frames a−d were taken 586, 736, and 1226 s and 4 h, respectively, after the temperature jump. Row B (HbC-Harlem) frames a−d were taken 240, 260, and 320 s and 24 h, respectively, after the temperature jump. Row C ($\alpha_2\beta_2^{E6V,T4S}$) frames a−d were taken 1800, 2200, and 3600 s and 20 h, respectively, after the temperature jump. Row D ($\alpha_2\beta_2^{E6V,T4Y}$) frames a−d were taken 240, 440, and 1240 s and 20 h, respectively, after the temperature jump. Row E ($\alpha_2\beta_2^{E6V,T4V}$) frames a−c were taken 150, 420, and 1920 s, respectively, after the temperature jump.

deoxy-HbS β4 variants, including HbS and HbC-Harlem in the deoxy form after a delay time in 1.0 M phosphate buffer at 22 °C following a temperature jump. These samples were preincubated for 1 h on ice using a sealed glass capillary tube mounted on a glass slide prior to the temperature jump. We found that a sealed glass capillary tube generates a much more uniform solution distribution compared to a glass slide with a coverslip, which generates an only ∼5−10 μm solution depth. In addition, this shallow solution depth on a slide with a coverslip inhibits vertical growth of fibers in favor of promoting lateral growth; fibers on such a slide can reach >10 μm in length, and DIC images of fibers and domains after a temperature jump of deoxy-HbS at 3.0 g/dL in 1.0 M phosphate buffer using the sealed capillary tube (30 μm path length, 0.3 mm width, and 50 mm length) are shown in Figure 2 (row A). Spherulitic, ovoid-shaped domains of deoxy-HbS were ∼3-fold shorter (∼30 μm in length for the major axis at 3.0 g/dL) in 1.0 M compared to those in 0.1 M phosphate buffer. Fibers in domains of HbS in 1.0 M phosphate buffer also had the highest density at the center and then grew outward to form ordered, elongated HbS fibers. Bending and branching of HbS fibers were not obvious in 1.0 M phosphate buffer, suggesting minimal heterogeneous nucleation during fiber elongation, and it took more than 3 h to observe elongated fibers that formed gels. The rate of elongation of fibers for 3.0 g/dL deoxy-HbS in 1.0 M phosphate buffer was 0.14 ± 0.029 μm/s (Figure 3), which is 9-fold slower than that for HbS in 0.1 M phosphate buffer.

Deoxy-HbC-Harlem fibers in 1.0 M phosphate buffer at 6.1 g/dL using the sealed capillary tube grew after nearly 4 min and formed ball-shaped domains (Figure 2, row B). The number of domains increased linearly as a function of time (Figure 4). An image of a single ball-shaped domain of HbC-Harlem is shown in Figure 5 (row A). The rate of fiber growth in a deoxy-HbC-Harlem domain was 0.105 ± 0.0096 μm/s, which is slightly slower than that of 3.0 g/dL deoxy-HbS under the same conditions. In addition, we observed large, clear, needlelike crystals from some of the HbC-Harlem domains after overnight incubation at room temperature (Figure 2, row B, frame d). Growth of these crystals was slow and continued for a few days in a low-phosphate buffer (*7*).

Next, we generated recombinant $\alpha_2\beta_2^{E6V,T4S}$ to further elucidate the effects of the β4Thr−β73Asp hydrogen bond interaction on domain and fiber formation. This amino acid change would be expected to modify β4−β73 hydrogen bond formation in HbS polymers since Ser has one fewer CH_3 group and its OH group is on the terminal CH_3 group compared to Thr in which the OH group is on an internal

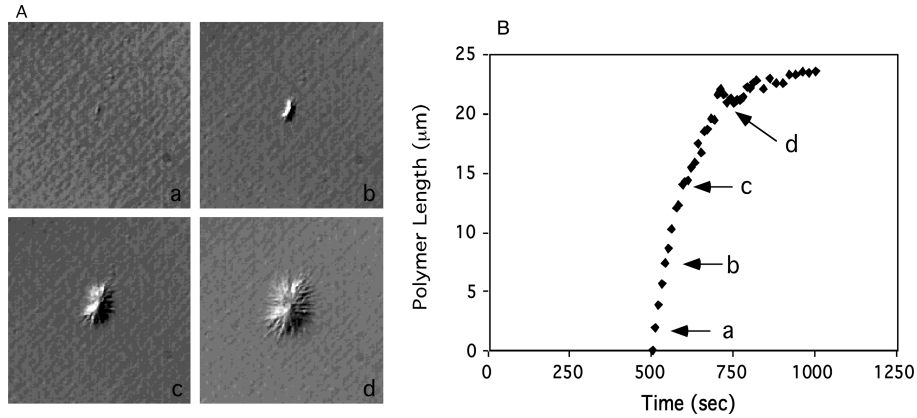

FIGURE 3: Time course of growth of fibers in a single domain of deoxy-HbS fibers in 1.0 M phosphate buffer using DIC microscopy. (A) DIC images of growing deoxy-HbS (3.0 g/dL) fibers in domains as a function of time in 1.0 M phosphate buffer. Frames a−d were taken at 510, 540, 595, and 730 s, respectively. (B) Growth rates of HbS fibers in a single domain were evaluated by counting pixel number (fiber length) as a function of time.

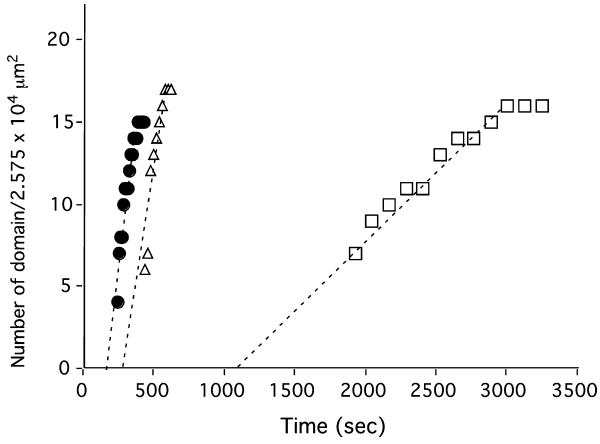

FIGURE 4: Time course for the increase in the number of domains for fibers of HbS variants in 1.0 M phosphate buffer using DIC microscopy. The increase in the number of domains for HbS β4 and β73 variants in the deoxy form in an area of 190 μm × 125 μm was measured as a function of time: (●) 6.1 g/dL HbC-Harlem, (□) 3 g/dL $\alpha_2\beta_2^{E6V,T4S}$, and (△) 4.2 g/dL $\alpha_2\beta_2^{E6V,T4Y}$.

CH_3 group. Oversaturated deoxy-$\alpha_2\beta_2^{E6V,T4S}$ at 3.0 g/dL in 1.0 M phosphate buffer had a longer delay time prior to polymerization than deoxy-HbS at 3.0 g/dL. After ~25 min, fibers formed as with deoxy-HbS, and the growth rate (0.016 ± 0.0036 μm/s) was one-ninth of that of HbS. Images of the single spherulitic domains were similar to those of HbS, but with a longer ovoid shape (Figure 2, row C, and Figure 5, row B). These elongated fibers did not generate crystals like HbC-Harlem after overnight incubation (Figure 2, row C, frame d).

We also engineered HbS containing a bulky β4 amino acid with an OH group (Tyr instead of Thr) and evaluated effects on fiber and domain formation. This amino acid change would be expected to affect the β4−β73 hydrogen bond more than Ser. Deoxy-$\alpha_2\beta_2^{E6V,T4Y}$ at 3.0 g/dL in 1.0 M phosphate buffer did not generate fibers after 1 h, but at 4.0 g/dL, visible fibers and domains formed after a delay time of 4 min. DIC images of fibers and domains looked like those from deoxy-HbC-Harlem. Images of fibers or multidomains and a single domain generated by deoxy-$\alpha_2\beta_2^{E6V,T4Y}$ as a function of time are shown in Figure 2 (row D) and Figure 5 (row C). The growth rate of domains from deoxy-$\alpha_2\beta_2^{E6V,T4Y}$ at 4.2 g/dL (0.112 ± 0025 μm/s) was slightly lower than that of deoxy-HbS at 3.0 g/dL. Domains stopped growing after achieving a length of ~30 μm after ~2 h at room temperature. In addition, clear, large, needlelike crystals were generated from some of the domains after overnight incubation at room temperature as shown for deoxy-HbC-Harlem (Figure 2, row D, panel d) and deoxy-$\alpha_2\beta_2^{E6V,D73L}$ (*7*). The number of domains for all of these HbS variants increased linearly as a function of time (Figure 4). These results indicate that $\alpha_2\beta_2^{E6V,T4S}$ and $\alpha_2\beta_2^{E6V,T4Y}$ inhibit normal β4−β73 hydrogen bond formation in HbS polymers, with inhibition by β4Tyr being stronger than that by β4Ser but weaker than that by β73Asn or β73Leu. In addition, deoxy-$\alpha_2\beta_2^{E6V,T4Y}$ generated straight, needle- and crystalline-like fibers forming ball-shaped domains like HbC-Harlem and $\alpha_2\beta_2^{E6V,D73L}$ in the deoxy form (*7*), not like β4Ser, which generated rodlike fibers like HbS or $\alpha_2\beta_2^{E6V,D73H}$ in the deoxy form (*7*). Fibers of $\alpha_2\beta_2^{E6V,T4S}$ and $\alpha_2\beta_2^{E6V,T4Y}$ appear to be like those of HbS and HbC-Harlem, respectively. DIC images of single-domain growth as a function of time show many growing fibers. HbS (Figure 3, panel A) and $\alpha_2\beta_2^{E6V,T4S}$ (Figure 5, row B) form an ovoid-shaped domain, while HbC-Harlem and $\alpha_2\beta_2^{E6V,T4Y}$ (Figure 5, rows A and C, respectively) form a ball-shaped domain with dynamic three-dimensional growth resulting in numerous nucleated fibers growing from a single cluster (Figure 5).

We next engineered $\alpha_2\beta_2^{E6V,T4V}$, which lacks an OH group and is expected to eliminate hydrogen bond formation with β73Asp. In addition, this change should enhance β6Val hydrophobicity at the A helix in the β chain. Interestingly, $\alpha_2\beta_2^{E6V,T4V}$ generated tiny particles or aggregates without a delay time after the temperature jump. Kinetics of aggregate formation using light scattering showed no delay time even at 0.3 g/dL. DIC images of amorphous aggregates of deoxy-$\alpha_2\beta_2^{E6V,T4V}$ at 0.5 g/dL are shown in Figure 2 (row E). These aggregates moved randomly in solution by Brownian movement in the glass capillary tube, and their shape and number did not change during incubation. The number of aggregates depends on concentration; the higher the concentration, the greater the number of aggregates. Some aggregates appeared to interact as a function of time (Figure 2, row E, frame c), and aggregates in 1.0 M phosphate buffer could be solubilized after dilution to 0.5 M phosphate, indicating they are not caused by denaturation. In addition, oxy as well as deoxy forms of $\alpha_2\beta_2^{E6V,T4V}$ generated amorphous aggregates (Figure 5, panel E, and Figure 2, panel E, respectively) like oxy-Hb

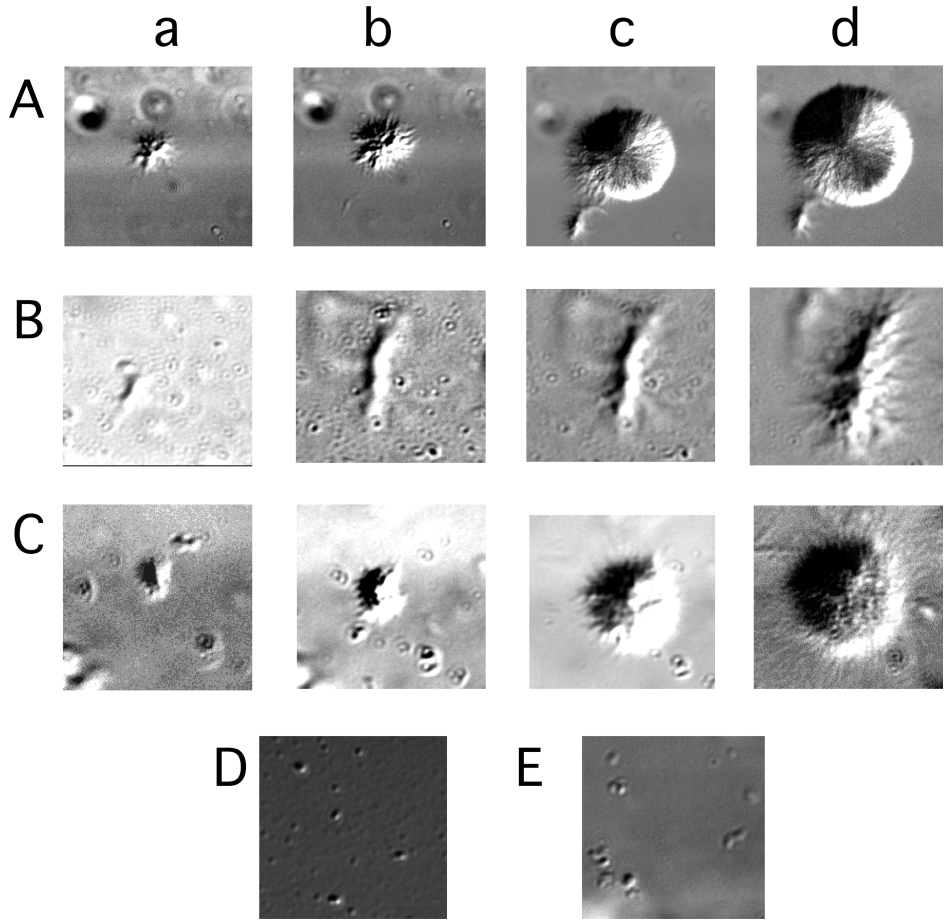

FIGURE 5: DIC images of growing single domains from HbS β73 and β4 variants and amorphous aggregates of oxy-HbS and oxy-$\alpha_2\beta_2^{E6V,T4V}$. DIC images of growth of single domains of deoxy forms of HbC-Harlem (row A), $\alpha_2\beta_2^{E6V,T4S}$ (row B), and $\alpha_2\beta_2^{E6V,T4Y}$ (row C) and oxy forms of HbS (panel D) and $\alpha_2\beta_2^{E6V,T4V}$ (panel E) in 1.0 M phosphate buffer (pH 7.4) at 22 °C were recorded as a function of time in a 30 μm × 30 μm area. Frames a−d of row A (6.1 g/dL, HbC-Harlem) were taken 240, 245, 260, and 420 s, respectively, after the temperature jump. Frames a−d of row B (3.0 g/dL, $\alpha_2\beta_2^{E6V,T4S}$) were taken 1680, 1920, 2640, and 4200 s, respectively, after the temperature jump. Frames a−d of row C (4.2 g/dL, $\alpha_2\beta_2^{E6V,T4Y}$) were taken 299, 379, 679, and 7479 s, respectively, after the temperature jump. Panels D and E are DIC images of generated amorphous aggregates of 10 g/dL oxy-HbS and 0.3 g/dL oxy-$\alpha_2\beta_2^{E6V,T4V}$, respectively, in 1.0 M phosphate buffer (pH 7.4) at 22 °C which formed instantly after the temperature jump, and their shape and size did not change for at least 10 min.

S at 10 g/dL (Figure 5, panel D). The critical concentration required to generate amorphous aggregates of deoxy- and oxy-$\alpha_2\beta_2^{E6V,T4V}$ (~0.3 g/dL) was also similar to that for $\alpha_2\beta_2^{E6V,D73H}$ (*7*) but ~10- and 35-fold lower than that for deoxy- and oxy-HbS, respectively. These results are in contrast to those of polymerization of $\alpha_2\beta_2^{E6V,D73L}$ in which polymer formation is inhibited compared to HbS (e.g., required a >5-fold higher concentration than HbS for polymerization) and is accompanied by a delay time prior to polymerization as measured by turbidity (*7*).

Kinetics of polymerization assessed by turbidity of oversaturated $\alpha_2\beta_2^{E6V,T4Y}$ and $\alpha_2\beta_2^{E6V,T4S}$ solutions exhibited a delay time prior to polymerization, and a delay time prior to domain formation was observed by DIC microscopy (Figures 3 and 4). The higher the hemoglobin concentration, the shorter the delay time. In contrast, deoxy-$\alpha_2\beta_2^{E6V,T4V}$ instantly aggregated without a delay time assessed by both turbidity and DIC. Solubilities of these HbS variants were measured at the plateau of polymerization following centrifugation. The solubility of deoxy-$\alpha_2\beta_2^{E6V,T4V}$ (0.22 ± 0.004 g/dL) was 10-fold lower than that of deoxy-HbS (2.1 ± 0.039 g/dL in 1.0 M phosphate buffer at pH 7.4 and 22 °C), while the solubilities of $\alpha_2\beta_2^{E6V,T4S}$ (2.31 ± 0.062 g/dL) and $\alpha_2\beta_2^{E6V,T4Y}$ (3.03 ± 0.094 g/dL) in the deoxy form increased 1.14- and 1.54-fold, respectively, compared to that of deoxy-HbS under the same conditions. The solubility of oxy-$\alpha_2\beta_2^{E6V,T4V}$ (0.235 ± 0.006 g/dL) was slightly higher than that of deoxy-$\alpha_2\beta_2^{E6V,T4V}$ but much lower than that of oxy-HbS (7.71 ± 0.203 g/dL) under the same conditions. Solubility and morphologic properties of HbS β4 and β73 variants in 1.0 M phosphate buffer (pH 7.4) as well as kinetic results assessed by turbidity and DIC compared to those of oxy- and deoxy-HbS are summarized in Table 1. These results suggest that enhanced hydrophobic interactions caused by β4Val and β6Val with other hydrophobic amino acids of adjacent HbS molecules (e.g., Ala, Phe, and Leu in the F helix) in deoxy-$\alpha_2\beta_2^{E6V,T4V}$ may disrupt the hydrogen bond with β73Asp like oxy-$\alpha_2\beta_2^{E6V,T4V}$ and oxy-HbS. This then might result in a loss of formation of nuclei following metastable liquid cluster formation and in additional hydrophobic interactions caused by β4Val, promoting generation of small, insoluble, amorphous aggregates in both oxy- and deoxy-$\alpha_2\beta_2^{E6V,T4V}$. These results are in contrast to those of deoxy-$\alpha_2\beta_2^{E6V,D73H}$ which may enhance the β4−β73 hydrogen bond in addition to the β6Val hydrophobic contacts, resulting in formation of spherulitic domains with HbS-like

Table 1: Kinetics and Domain Properties of HbS β4 and β73 Variants and Their Solubilities Compared to Those of Oxy- and Deoxy-HbS in 1.0 M Phosphate Buffer[a]

HbS and HbS variant	delay time prior to polymerization	domain shape	fiber image	solubility (g/dL)
deoxy-HbS	+	ovoid-like	14-stranded	2.10 ± 0.039
oxy-HbS	−	none	amorphous aggregates	7.71 ± 0.203
deoxy-HbC-Harlem	+	ball-like	double-stranded	3.26 ± 0.096 (*7*)
deoxy-$\alpha_2\beta_2^{E6V,D73L}$	+	ball-like	HbC-Harlem-like	3.5 ± 0.03 (*7*)
deoxy-$\alpha_2\beta_2^{E6V,T4Y}$	+	ball-like	HbC-Harlem-like	3.03 ± 0.094
deoxy-$\alpha_2\beta_2^{E6V,D73H}$	+	ovoid-like	HbS-like	0.29 ± 0.003 (*7*)
deoxy-$\alpha_2\beta_2^{E6V,T4S}$	+	ovoid-like	HbS-like	2.31 ± 0.006
deoxy-$\alpha_2\beta_2^{E6V,T4V}$	−	none	amorphous aggregates	0.220 ± 0.004
oxy-$\alpha_2\beta_2^{E6V,T4V}$	−	none	amorphous aggregates	0.235 ± 0.006

[a] Domain properties and the solubility of HbS and HbS variants were evaluated in 1.0 M phosphate buffer (pH 7.4) at 22 °C (*7*), and the solubility was determined by centrifugation after completion of polymerization measured by the turbidity method. The presence of a delay time prior to polymerization was determined by turbidity measurements (*7*).

nucleated fibers and with reduced solubility like $\alpha_2\beta_2^{E6V,T4V}$ (*7*). These results indicate that the hydrogen bond between β4 and β73 amino acids in addition to β6Val hydrophobicity plays a critical role in the formation of a single domain containing numerous ordered fibers like deoxy-HbS or HbC-Harlem.

DISCUSSION

Phosphate Concentration Dependency for Domain and Fiber Formation of HbS. Progress of HbS fiber and domain formation in vitro can be monitored by a variety of techniques (*2*), and results depend on experimental conditions. For instance, size and growth rates of fibers and domains of deoxy-HbS using laser photolysis are dependent on the illuminated area for converting CO-HbS to the deoxy form (*15, 17*). In addition, changes in photolytic intensity altered domain growth rates and structure, and the number of spherulitic domains increased linearly as a function of time (*16, 17*). Using DIC images of deoxy-HbS fiber and domain formation, we found after a temperature jump that size and growth rates of fibers of HbS polymers were phosphate concentration-dependent but that fiber structure and domain shape resulting from growth of fibers from a central region via liquid−solid phase transition were similar in both 1.0 and 0.1 M phosphate buffers. Our results showing time-dependent increases in the number of spherulitic domains of deoxy-S fibers in 1.0 M phosphate buffer are consistent with those of Galkin and Vekilov using photolysis in 0.15 M phosphate buffer (*16, 17*). Electron microscopic structural analyses showed that HbS polymers made in 0.05 or 1.5 M phosphate buffer were identical, and three-dimensional reconstruction of micrographs of frozen hydrated fibers demonstrated identical structures formed in low- versus high-phosphate buffers (*27*). However, with higher phosphate concentrations, we found that domain size was smaller and domain number increased exponentially, indicating that nucleation rates increase as phosphate concentration increases. Increases in phosphate concentration could reduce free water to keep the protein fully hydrated, influencing aggregation behavior of monomers and polymers of HbS. These results suggest that formation of critical metastable nuclei by oversaturated monomers within domains for deoxy-HbS polymers is promoted by increasing the phosphate concentration, resulting in reduction of oversaturated deoxy-HbS monomers to associate with polymers. Thus, increasing the phosphate concentration may lead to generation of short fibers with increasing numbers of domains and slow growth of each fiber. In spite of these differences, use of 1.0 M phosphate buffer instead of 0.1 or 0.15 M phosphate buffer, which is more physiological, facilitates comparative studies of polymerization of HbS and its variants by reducing the Hb concentration required for polymerization. Such studies lead to an improved understanding of HbS polymerization.

Role of the β4Thr−β73Asp Hydrogen Bond in HbS Domain Formation from a Multinucleate-Containing Cluster. The time course for deoxy-HbS polymer formation shows an abrupt initiation after a characteristic delay time, which is extremely sensitive to hemoglobin concentration. This process is called homogeneous nucleation and takes place in bulk solution (*2*). With homogeneous nucleation, small aggregates or oligomers made by deoxy-HbS molecules are unstable relative to monomers, and the addition of an oversaturated monomer to the oligomer produces a metastable aggregate (*2*). Once a certain size is reached, a "critical nucleus" is formed; however, further addition of monomers produces more stable polymers. Such small critical nuclei which act as a cluster or nucleus for further polymerization cannot be observed by DIC microscopy, although stable polymers and domains can be detected. After longer periods, these networks or polymer domains assume a spherulitic form, from which polymers radiate uniformly in all directions. HbS polymer domains are spherulitic and are visible as Maltese crosses, whereas domains of HbC-Harlem, $\alpha_2\beta_2^{E6V,D73L}$, and $\alpha_2\beta_2^{E6V,T4Y}$ are three-dimensional ball-shaped domains with uniform growth of many fibers from a single cluster after a delay time (Table 1).

Galkin et al. (*17*) recently reported that nucleation of HbS polymers proceeds via a precursor involving a metastable mesoscopic cluster of a dense liquid phase in a crowded HbS solution. They suggested that homogeneous nucleation of HbS polymers occurs within a cluster as a precursor phase (*17, 28*). Nucleation of crystalline nuclei also was suggested to proceed by a two-step process: a droplet of dense liquid forms, within which a crystalline nucleus appears due to the ordering of a certain number of molecules (*18, 29*). In our DIC experiments, we did not detect any dropletlike structures involved in liquid−liquid clusters prior to formation of domains (*30*). Nonetheless, it is conceivable that randomly dense clusters of deoxy-HbS and -$\alpha_2\beta_2^{E6V,T4S}$ as well as deoxy-HbC-Harlem and $\alpha_2\beta_2^{E6V,T4Y}$ in an oversaturated solution may lead to generation of numerous ordered fibers emerging from each cluster

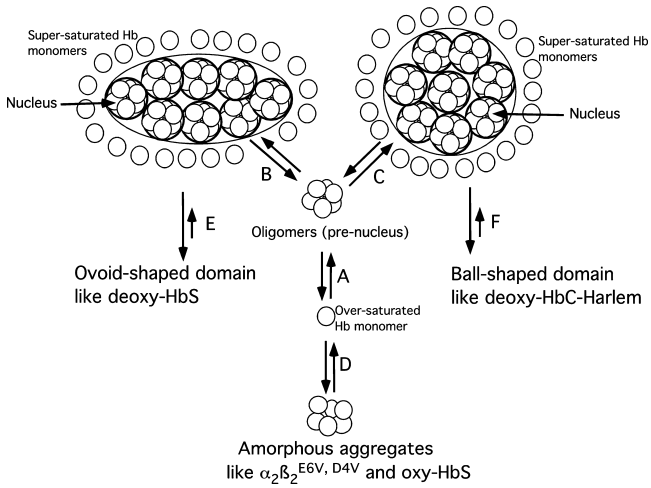

FIGURE 6: Model for formation of two different multinuclei metastable liquid domains (ovoid-like and ball-like) prior to fiber vs amorphous aggregate formation in supersaturated solutions of HbS and its variants. Supersaturated HbS, HbC-Harlem, $\alpha_2\beta_2^{E6V,D73H}$, $\alpha_2\beta_2^{E6V,D73L}$, $\alpha_2\beta_2^{E6V,T4S}$, and $\alpha_2\beta_2^{E6V,T4Y}$ in the deoxy form generate an equilibrium between monomers and self-associated oligomers which facilitate formation of prenuclei (reaction A). A metastable, single, multinucleated dense liquid cluster is generated prior to fiber formation. Formation in a supersaturated solution of either a ball-shaped (reaction C) or ovoid-shaped dense liquid cluster (reaction B) occurs, which serves as a precursor to formation of multihomogeneous nuclei. Ball-shaped clusters like those of $\alpha_2\beta_2^{E6V,D73L}$ and $\alpha_2\beta_2^{E6V,T4Y}$ generate ball-shaped domains exhibiting growth of HbC-Harlem-like fibers (reaction F), while ovoid-shaped dense liquid clusters generate ovoid-shaped domains like $\alpha_2\beta_2^{E6V,D73H}$ or $\alpha_2\beta_2^{E6V,T4S}$ (reaction E) and grow like HbS fibers. In contrast, supersaturated monomeric oxy- and deoxy-$\alpha_2\beta_2^{E6V,T4V}$ with increased β4 hydrophobicity and weakened β4 hydrogen bond interactions with β73Asp form small, amorphous aggregates, thereby inhibiting formation of nuclei for fiber growth (reaction D).

instead of a single, nucleated fiber from each metastable cluster. This dense liquid cluster may represent an intermediate phase from the liquid to solid phase transition during formation of nuclei and may result in formation of many ordered fibers with uniform growth rates in a single domain. This is in contrast to a single nucleus in a single cluster for crystal formation of protein (*29*).

We propose a working model for formation of two different cluster types: ovoid- and ball-shaped containing multiple oligomers that function as nuclei prior to formation of either HbS-like (14-stranded) or HbC-Harlem-like (double-stranded) fibers instead of forming amorphous aggregates (Figure 6). The model is highly speculative at this time and requires detailed molecular and structural studies defining the nature of fibers formed from these two different proposed cluster types. Ovoid-shaped liquid clusters may promote metastable nuclei like deoxy-HbS (Figure 3, frame A) and $\alpha_2\beta_2^{E6V,T4S}$ (Figure 5, row B) compared to ball-shaped domains made from ball-shaped clusters like deoxy-HbC-Harlem and deoxy-$\alpha_2\beta_2^{E6V,T4Y}$ (Figure 5, rows A and C, respectively) or deoxy-$\alpha_2\beta_2^{E6V,D73L}$ (*7*). Surrounding monomers near an ovoid-shaped cluster might facilitate interaction with growing ends of single nucleated fibers spontaneously to form ordered, elongated fibers. In contrast, a ball-shaped liquid cluster would generate a ball-shaped domain with uniform growth rates of straight fibers. We propose that ovoid-shaped clusters generate 14-stranded fibers while ball-shaped clusters generate double-stranded fibers. Metastable cluster formation would depend on the surface free energy of a liquid shell cluster, which would be controlled by protein−protein interactions of nuclei and monomers. The size and rate of formation of nuclei then would depend on the strength of the hydrogen bond between β4Thr and β73Asp and the balance between the hydrogen bond and the β6Val hydrophobic interactions in the polymer. When the balance of contacts of hemoglobin molecules with water molecules becomes more hydrophobic as in oxy- and deoxy-$\alpha_2\beta_2^{E6V,T4V}$, then oversaturated hemoglobin molecules would facilitate initiation of self-aggregation to form insoluble, amorphous aggregates without a delay time. Liquid cluster formation may depend on in vivo as well as in vitro conditions (e.g., solution composition, temperature, flow and hydrodynamics of solution, etc.). Additional parameters for nucleation in a single, dense liquid cluster prior to HbS polymerization other than HbS concentration and solubility in RBCs may affect domain formation. Definition of these parameters and validation of the cluster model containing multiple nuclei should provide new insights into the sickling process as well as improve our understanding of diseases in which protein fibers are formed.

ACKNOWLEDGMENT

We thank F. Ferrone and T. Asakura for valuable suggestions and discussions and also acknowledge J. Fithian for editorial assistance with the manuscript. We also thank C. F. Mitchell for technical help with Hb fiber image analysis using DIC microscopy.

REFERENCES

1. Bunn, H. F., and Forget, B. G. (1996) *Hemoglobin: Molecular and Clinical Aspects*, Sanders, Philadelphia.
2. Eaton, W. A., and Hofrichter, J. (1990) Sickle cell hemoglobin polymerization. *Adv. Protein Chem. 40*, 63–279.
3. Dykes, G. W., Crepeau, R. H., and Edelstein, S. J. (1979) Three-dimensional reconstruction of the 14-filament fibers of hemoglobin S. *J. Mol. Biol. 130*, 451–472.
4. Padlan, E. A., and Love, W. E. (1985) Refined crystal structure of deoxyhemoglobin S. I. Restrained least-squares refinement at 3.0-Å resolution. *J. Biol. Chem. 260*, 8272–8279.
5. Harrington, D. J., Adachi, K., and Royer, W. E. (1997) The high resolution crystal structure of deoxyhemoglobin S. *J. Mol. Biol. 272*, 398–407.
6. Ivanova, M., Jasuja, R., Krasnosselskaia, L., Josephs, R., Wang, Z., Ding, M., Horiuchi, K., Adachi, K., and Ferrone, F. A. (2001) Flexibility and nucleation in sickle hemoglobin. *J. Mol. Biol. 314*, 851–861.
7. Adachi, K., Ding, M., Wehrli, S., Reddy, K. S., Surrey, S., and Horiuchi, K. (2003) Effects of different β73 amino acids on formation of 14-stranded fibers of Hb S versus double-stranded crystals of Hb C-Harlem. *Biochemistry 42*, 4476–4484.
8. Ferrone, F. A., Hofrichter, J., and Eaton, W. A. (1985) Kinetics of sickle hemoglobin polymerization. I. Studies using temperature-jump and laser photolysis techniques. *J. Mol. Biol. 183*, 591–610.
9. Ferrone, F. A., Hofrichter, J., and Eaton, W. A. (1985) Kinetics of sickle hemoglobin polymerization. II. A double nucleation mechanism. *J. Mol. Biol. 183*, 611–631.
10. Eaton, W. A., and Hofrichter, J. (1995) The biophysics of sickle cell hydroxyurea therapy. *Science 268*, 1142–1143.
11. Ferrone, F. A., Ivanova, M., and Jasuja, R. (2002) Heterogeneous nucleation and crowding in sickle hemoglobin: An analytic approach. *Biophys. J. 82*, 399–406.
12. White, J. G., and Heagan, B. (1970) The fine structure of cell-free sickled hemoglobin. *Am. J. Pathol. 58*, 1–17.
13. Hofrichter, J., Hendricker, D. G., and Eaton, W. A. (1973) Structure of hemoglobin S fibers: Optical determination of the molecular orientation in sickled erythrocytes. *Proc. Natl. Acad. Sci. U.S.A. 70*, 3604–3608.

14. Samuel, R. E., Salmon, E. D., and Briehl, R. W. (1990) Nucleation and growth of fibres and gel formation in sickle cell haemoglobin. *Nature 345*, 833–835.
15. Briehl, R. W. (1995) Nucleation, fiber growth and melting, and domain formation and structure in sickle cell hemoglobin gels. *J. Mol. Biol. 245*, 710–723.
16. Galkin, O., and Vekilov, P. G. (2004) Mechanisms of homogeneous nucleation of polymers of sickle cell anemia hemoglobin in deoxy state. *J. Mol. Biol. 336*, 43–59.
17. Galkin, O., Nagel, R. L., and Vekilov, P. G. (2007) The kinetics of nucleation and growth of sickle cell hemoglobin fibers. *J. Mol. Biol. 365*, 425–439.
18. Vekilov, P. G. (2007) Sickle-cell haemoglobin polymerization: Is it the primary pathogenic event of sickle-cell anaemia? *Br. J. Haematol. 139*, 173–184.
19. Adachi, K., and Asakura, T. (1980) Polymerization of deoxyhemoglobin CHarlem (β6Glu replaced by Val, β73Asp replaced by Asn). The effect of β73 asparagine on the gelation and crystallization of hemoglobin. *J. Mol. Biol. 144*, 467–480.
20. Adachi, K., Ding, M., Surrey, S., Rotter, M., Aprelev, A., Zakharov, M., Weng, W., and Ferrone, F. A. (2006) The Hb A Variant (β73Asp→Leu) Disrupts Hb S Polymerization by a Novel Mechanism. *J. Mol. Biol. 362*, 528–538.
21. Akbar, M. G., Tamura, Y., Ding, M., Ding, H., Rosenblatt, M. M., Reddy, K. S., Surrey, S., and Adachi, K. (2006) Inhibition of hemoglobin S polymerization in vitro by a novel 15-mer EF-helix β73 histidine-containing peptide. *Biochemistry 45*, 8358–8367.
22. Carrell, R. W., and Lomas, D. A. (1997) Conformational disease. *Lancet 350*, 134–138.
23. Kelly, J. W. (2000) Mechanisms of amyloidogenesis. *Nat. Struct. Biol. 7*, 824–826.
24. Koo, E. H., Lansbury, P. T., Jr., and Kelly, J. W. (1999) Amyloid diseases: Abnormal protein aggregation in neurodegeneration. *Proc. Natl. Acad. Sci. U.S.A. 96*, 9989–9990.
25. Shen, T. J., Ho, N. T., Simplaceanu, V., Zou, M., Green, B. N., Tam, M. F., and Ho, C. (1993) Production of unmodified human adult hemoglobin in *Escherichia coli*. *Proc. Natl. Acad. Sci. U.S.A. 90*, 8108–8112.
26. Adachi, K., Konitzer, P., Kim, J., Welch, N., and Surrey, S. (1993) Effects of β6 aromatic amino acids on polymerization and solubility of recombinant hemoglobins made in yeast. *J. Biol. Chem. 268*, 21650–21656.
27. Wang, Z., Kishchenko, G., Chen, Y., and Josephs, R. (2000) Polymerization of deoxy-sickle cell hemoglobin in high-phosphate buffer. *J. Struct. Biol. 131*, 197–209.
28. Pan, W., Galkin, O., Filobelo, L., Nagel, R. L., and Vekilov, P. G. (2007) Metastable mesoscopic clusters in solutions of sickle-cell hemoglobin. *Biophys. J. 92*, 267–277.
29. Kashchiev, D., Vekilov, P. G., and Kolomeisky, A. B. (2005) Kinetics of two-step nucleation of crystals. *J. Chem. Phys. 122*, 244706.
30. Galkin, O., Chen, K., Nagel, R. L., Hirsch, R. E., and Vekilov, P. G. (2002) Liquid-liquid separation in solutions of normal and sickle cell hemoglobin. *Proc. Natl. Acad. Sci. U.S.A. 99*, 8479–8483.

BI800149U